Competitive Reactions of Interstrand and Intrastrand DNA-Pt Adducts: A Dinuclear-Platinum Complex Preferentially Forms a 1,4-Interstrand Cross-Link Rather than a 1,2 Intrastrand Cross-link on Binding to a GG 14-Mer Duplex

Susan J. Berners-Price,*[a] Murray S. Davies,[c] John W. Cox,[b] Donald S. Thomas,[a] and Nicholas Farrell*[b]

Abstract: A study of the kinetics and mechanism of the reaction between the dinuclear Pt complex [{*trans*-PtCl-$(NH_3)_2$}$_2$(μ-$NH_2(CH_2)_6NH_2$)]$^{2+}$ (**1**) and the 14-mer duplex 5′-d(ATACAT-G(7)G(8)TACATA)-3′ · 5′-d(TATG(25)-TACCATG(18)TAT)-3′ is reported. [^{1}H,^{15}N]-HSQC NMR was used to follow the reaction at 298 K, pH 5.4. The product is primarily the 5′–5′ 1,4-interstrand cross-link between G(8) and G(18) bases and exists in two conformational forms. No evidence for the possible 1,2-intrastrand G(7)G(8) adduct was seen, confirming the preferential formation of interstrand cross-links by these dinuclear complexes. An initial electrostatic association of ^{15}N-**1** with the duplex is indicated by changes in its ^{1}H/^{15}N chemical shifts, followed by aquation of **1** to form the monoaqua monochloro species **2**, with a rate constant of $4.00 \pm 0.03 \times 10^{-5}$ s^{-1}. Monofunctional binding to the duplex occurs primarily at G(8), the 3′ base of the nucleophilic GG grouping, with a rate constant of 1.5 ± 0.7 M^{-1}s^{-1}. Changes in the ^{1}H/^{15}N shifts indicate there is an electrostatic interaction between the unbound {PtN_3Cl} group of the monofunctional adduct and the duplex. No peaks for a transient aquated monofunctional species are seen and closure of **3** to form the 1,4-G(8)G(18) interstrand cross-link (**5**) was treated as direct, with a rate constant of $4.47 \pm 0.06 \times 10^{-5}$ s^{-1}. The G(8)G(18) cross-link was confirmed from analysis of the NOESY NMR spectrum of the final product. Structural perturbations for the 1,4-interstrand cross-link extend over approximately four base-pairs and are similar to those found for a 1,4-interstrand cross-link with a shorter 8-mer -GTAC- sequence. A major distortion was evident for the 5′T (T(17)) adjacent to the platinated G(18), consistent with the findings from the use of chemical probes to investigate the conformation of 1,4-interstrand cross-links.

Keywords: antitumor agents · DNA · kinetics · NMR spectroscopy · platinum

Introduction

The dinuclear Pt complex [{*trans*-$PtCl(NH_3)_2$}$_2$(μ-NH_2-$(CH_2)_6NH_2$)]$^{2+}$ (1,1/t,t ($n = 6$), **1**, Scheme 1) is the prototype of a series of multinuclear anticancer platinum compounds linked by variable length diamine chains.[1] The development of these compounds was driven by the hypothesis that complexes with distinct DNA binding mechanisms may

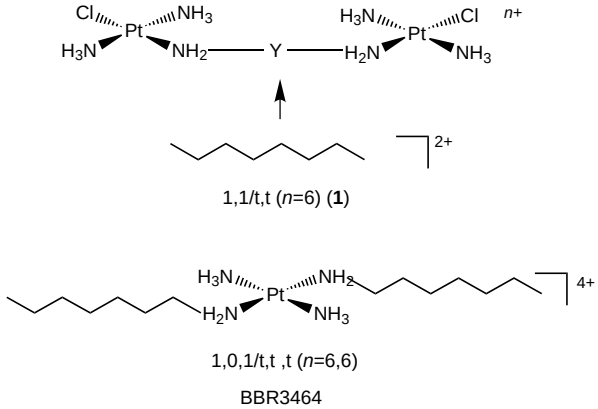

Scheme 1. General structure diagram for di- and trinuclear Pt complexes.

[a] Prof. S. J. Berners-Price, D. S. Thomas
Department of Chemistry
University of Western Australia
35 Stirling Hwy, Crawley, WA 6009 (Australia)
Fax: (+61) 8-9380-1005
E-mail: sbp@chem.uwa.edu.au

[b] Prof. N. Farrell, Dr. J. W. Cox
Department of Chemistry
Virginia Commonwealth University
Richmond, VA 23284-2006, (USA)
Fax: (+1) 804-828-8599
E-mail: nfarrell@saturn.vcu.edu.au

[c] Dr. M. S. Davies
School of Pharmacy and Molecular Sciences
James Cook University
Townsville QLD 4811 (Australia)

Supporting information for this article is available on the WWW under http://www.chemeurj.org/ or from the author.

  0947-6539/03/0903-0713 $ 20.00+.50/0

exhibit unique biological activity in comparison to the current mononuclear clinically-used agents.[1, 2] One member of this series, the trinuclear $[(trans\text{-}PtCl(NH_3)_2)_2\{\mu\text{-}trans\text{-}Pt(NH_3)_2(NH_2(CH_2)_6NH_2)_2\}]^{4+}$, (1,0,1/t,t,t $(n=6,6)$ or BBR3464) was advanced to Phase II clinical trials in ovarian, gastric, and lung cancer after showing responses to colon and pancreatic cancers in Phase I trials.[3–5]

Both of these complexes have the generic structure below, representing only one structurally distinct sub class of polynuclear platinum compounds.(Scheme 1).[1, 2, 6]

Incorporation of charge into the linking backbone, either through a non covalent platinum center, as in BBR3464, or a linear polyamine such as spermidine or spermine, results in significantly increased cytotoxic and antitumor potency relative to the "simple" alkanediamine-bridged dinuclear compounds such as **1**.[7–9]

The DNA binding profiles for these bifunctional platinating agents, especially the formation of long-range (Pt – Pt) interstrand cross-links, are notably different from those found for cisplatin and other mononuclear platinum(II) compounds.[1, 7] The flexibility of the bridging group allows for the formation of a number of different cross-links, while classically, bifunctional mononuclear compounds are restricted in the number and type of cross-links they can form.[1, 9, 10] Also, the extent of interstrand cross-linking appears to be dependent on the overall charge of the complex, rather than on the distance between the platinating coordination spheres.[9]

This contribution reports on a continuation of our studies into the examination of solution chemistry and DNA interactions of **1** and BBR3464 by using [^{1}H,^{15}N]-HSQC NMR spectroscopy.[11, 12] The [^{1}H,^{15}N] HSQC NMR technique is especially useful for following the reactions of the di- and trinuclear platinum am(m)ine complexes, because ^{15}N-labeling of both $^{15}NH_2$ and $^{15}NH_3$ groups is possible.[11] The NH_2 and NH_3 regions of the [^{1}H,^{15}N] 2D NMR spectra are well separated, and reaction courses can be followed independently in each region.

In this work, our general strategy has been to understand the dinuclear system first. A study and comparison of the trinuclear system then allows delineation of specific contributions of the central charged moiety in influencing interactions with target molecules. Previously we have studied the kinetics and mechanism of the binding of **1** to the self-complementary 12 mer duplex 5′-{d(ATATGTACATAT)$_2$} (**II**), in which the preferred bifunctional cross-link is a 1,4-interstrand 5′ – 5′ GG adduct.[12] This paper describes a study of the binding of **1** to the 14-base pair duplex 5′-d(ATACATGGTACATA)-3′ · 5′-d(TATGTACCATGTAT)-3′ (**I**). The formation of platinated adducts at the GG site of duplex **I** has also been studied for cisplatin[13] as well as for *cis*-$[PtCl_2(NH_3)$(2-picoline)$]$,[14] and $[PtCl(dien)]^+$.[15] The sequence offers three possible bifunctional binding sites for **1**, a 1,2-intrastrand GG adduct and two 1,4-interstrand GG adducts that differ in the direction (5′ – 5′ versus 3′ – 3′) of the cross-link (Scheme 2). This, therefore, provides the opportunity to examine the preference of the drug towards formation of these adducts in a competitive manner. Sequencing studies using polymerase inhibition assays showed that dinuclear

Scheme 2. Possible cross-links of **1** on **I**.

platinum compounds may bind at intrastrand GG sites, formally similar to that of cisplatin.[16] However, the interpretation of adduct structure by examination of sequence stop sites is equivocal. Whereas stop sites seen at GG sites are reasonably attributed to an intrastrand adduct, even sequences such as -GGCG- may give a variety of binding modes, even for cisplatin, contributing to polymerase inhibition.[16] In the case of long-range cross-links, this problem is exacerbated, because while the adduct on one strand inhibiting polymerase will produce a stop site, it is not possible by standard assays to determine where the second platination site occurs behind the polymerase inhibition site.[16]

The use of the duplex **I** also gives the opportunity to examine and compare changes in conformation brought about by Pt drug binding, because the NMR structures of both the free duplex **I** and its cisplatin adduct are known.[17] The assignment of the ^{1}H NOESY spectrum of the final product is described and shows that the 5′ – 5′ 1,4-interstrand G(8) – G(18) cross-link of **1** is the major product species and exists in two conformational forms.

Results

The preparation of ^{15}N-labeled $[\{trans\text{-}PtCl(NH_3)_2\}_2(\mu\text{-}NH_2(CH_2)_6NH_2)]^{2+}$ (**1**) and the characterization of its hydrolysis products by [^{1}H,^{15}N]-HSQC NMR spectroscopy have been described previously.[11] The formation of a 1,4-interstrand DNA cross-link by **1** has been examined on the 12-mer self complementary sequence 5′-d(ATATGTACATAT)-3′ (**II**).[12] Here, our studies are extended to examine the competitive binding preferences of **1** on 5′-d(ATACATGGTACATA)-3′ · 5′-d(TATGTACCATGTAT)-3′ (**I**), a sequence that offers a 1,2-intrastrand as well as two possible 1,4-interstrand GG binding modes. In general, the major features are as observed previously,[12] that is, 1) pre-association through hydrogen-bonding and electrostatic interactions, 2) monofunctional binding followed by 3) bifunctional adduct closure (Scheme 3). As in the previous study, a pH of 5.4 was chosen for the reaction. This pH lies 0.2 pH units below the p*K*a value of the monoaqua chloro form **2** (5.62),[11] allowing a more meaningful comparison with previous DNA platination reactions of duplex **I** by cisplatin[13, 18] that were carried out at pH 6.0 (p*K*a of *cis*-$[PtCl(NH_3)_2(H_2O)]^+$ is 6.41[19]).

Reaction of ^{15}N-1 with duplex I:

The pre-binding step: electrostatic association and aquation: Pre-association is indicated by the fact both ^{1}H and ^{15}N shifts of ^{15}N-**1** are slightly deshielded in the presence of duplex **I**, (Pt–NH_3 $\Delta\delta$ ^{1}H 0.04 ppm, ^{15}N 0.4 ppm Pt–NH_2 $\Delta\delta$ ^{1}H 0.03 ppm) when compared to a spectrum of a control solution of ^{15}N-**1** in the same phosphate buffer at the same pH

0947-6539/03/0903-0714 $ 20.00+.50/0 *Chem. Eur. J.* **2003**, *9*, No. 3

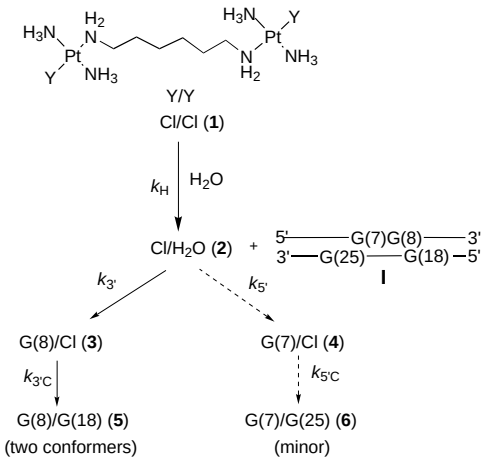

Scheme 3. Reaction pathway **1** + **I**.

(Table 1). The deshielding is similar to that observed in the reaction of ^{15}N-**1** with the self-complementary sequence **II** under similar conditions.[12] A notable difference is that the Pt–NH_3 peak has an unsymmetrical line that becomes more evident as the reaction proceeds (e.g. Figure 1c and d), appearing as two overlapped peaks of equal intensity.

Table 1. ^{1}H and ^{15}N shifts for intermediates observed during the reaction of **1** with the duplex 5′-d(ATACATG(7)G(8)TACATA)·3′-d(TATG(25)TACCATG(18)TAT) (**I**) at pH 5.4, 298 K.[a]

Species	Label	Pt–NH_3			Pt–NH_2
1,1,t,t ($n=6$)		δ^1H	δ^{15}N	δ^1H	δ^{15}N (*trans* ligand)
Y,Y′ = Cl	**1**	3.90	−64.2	5.06	−47.1(Cl)
		(3.86)	(−64.6)	(5.03)	(−47.0)
Y = Cl, Y′ = OH_2	**2**	[b]	[b]	[b]	(Cl)[b]
		4.21	−62.0	[c]	[c](OH_2)
		(4.00)	(−62.6)		
Y = N7 G(8), Y′ = Cl	**3**	3.95	−64.4	ca. 5.08[d]	−47.1 (Cl)
		4.17	−59.9	5.14–5.17[d]	−47.1 (N7G)
Y = N7 G(7), Y′ = Cl	**4**	3.95	−64.4	ca. 5.08[d]	−47.1(Cl)
		4.30	−61.0	5.14–5.17[d]	−47.1 (N7G)

[a] ^{1}H referenced to TSP, ^{15}N referenced to $^{15}NH_4Cl$ (external), δ in ^{15}N dimension ±0.2 ppm. ^{1}H and ^{15}N shifts for **1** and **2** in 15 mM phosphate buffer pH 5.4 in the absence of DNA are shown in parentheses. [b] Assumed to be concealed by peaks for **1**. [c] NH_2 peak for **2** is expected at δ 4.88/−62.2 at pH 5.4;[12] this is too close to H_2O to resolve at this concentration (*ca* 40 μM). [d] Pt–NH_2 peaks for **3** and **4** can not be distinguished; in both cases the Pt–NH_2 peak for the unbound {PtN_3Cl} group is assumed to be partially overlapped with that of **1**.

Further evidence for electrostatic association can be found on careful inspection of the ^{1}H NMR spectrum of the duplex before and immediately after addition of ^{15}N-**1**. Peaks in the aromatic, imino, and thymine methyl regions of the spectrum are readily assignable based on the published ^{1}H data for the duplex.[17] At least three peaks in these regions exhibited shifts of >0.01 ppm on addition of ^{15}N-**1**. Peak overlap precludes an unambiguous assignment but these are likely to be either A10 or A20 H2 ($\Delta\delta$ − 0.026 ppm), A10 or A20 H8 ($\Delta\delta$ + 0.035 ppm), and A12 or A14 H8 ($\Delta\delta$ + 0.025 ppm).

The deshielding of the Pt–NH_3 peak for the monoaqua monochloro species (**2**) ($\Delta\delta$ ^{1}H 0.21 ppm and ^{15}N 0.6 ppm) is also identical to that observed on binding to the self complementary sequence **II** under the same conditions,[12] indicating a similar electrostatic interaction with the DNA. The peak for **2** is too low in intensity to determine whether the line shape is unsymmetrical as is for **1**. The aquated species accounts for only 0.8% of the Pt–NH_3 species after 14 min (compared to 3% for the reaction with the 12-mer sequence **II**[12]); this is due to a more rapid formation of the monofunctional adduct.

Monofunctional binding step: The concentration of **1** decreases to 50% of its original concentration in about 5 h. Strong downfield shifts are diagnostic of platinated guanine.[12] The enhanced nucleophilicity of GG sites over isolated guanines results in preferential monofunctional platination at G(8) and G(7) over the G(18) or G(25) sites. Peaks assignable to the 3′G monofunctional adduct (G(8), **3**) were already visible in the first spectrum (14 min). Figure 1a shows the spectrum after 1.5 h. The peak at δ 4.17/−59.9 (labeled **3a** in Figure 1) is assigned to the Pt–$(NH_3)_2$ group coordinated to the G(8) N7 of the duplex, while the uncoordinated Pt–$(NH_3)_2$ group is assigned to the second peak (δ 3.95/−64.4, **3b**) because of its very similar shift to **1** (δ 3.90/−64.2). Assignment of this species, as the 3′G monofunctional adduct is based on the NOESY spectrum of the final product, which shows that the major adduct is a 1,4 G(8)G(18) interstrand cross-link. Further support for these conclusions comes from the reaction between cisplatin and the same sequence **I**, for which an excess of 90% of platination was found at the GG site with preferential monoadduct formation at the 3′-site.[13, 17]

After about 30 min a new peak appeared at δ 4.30/−61.1 (**4a**, Figure 1a), reasonably assigned to the 5′G monofunctional adduct **4** coordinated to the G(7) N7. Given that the shift of the uncoordinated Pt–$(NH_3)_2$ group of the monofunctional adduct is insensitive to the nature of the sequence (**I** or **II**), it is reasonable to assume that the partner peak is coincident with that of **3**.[20]

In the Pt–NH_2 region a broad peak at about δ 5.15/−47.1 has a time dependent profile consistent with that of a monofunctional adduct. The ^{1}H shift is slightly more strongly deshielded than for the monofunctional adduct with duplex **II** (δ 5.12)[12] and has an unsymmetrical line-shape that provides some evidence for overlap of peaks for the two monofunctional adducts [3′G (G(8)) and 5′G (G(7))]. Time dependent changes in the peak volumes in the $^{15}NH_2$ and $^{15}NH_3$ regions indicate that a second ^{1}H/^{15}N peak, due to at least one of the four NH_2 protons of **3** (and **4**), is overlapped with the peak for **1**.

In the aromatic region of the ^{1}H spectrum (Figure 2a), a peak at δ 8.55 is assigned to the H8 of the coordinated G residue of **3**, since it is visible before any peaks for product are observed in the [^{1}H,^{15}N]-HSQC NMR spectra. Further, at 1 h the relative ratio of **3**:**4** is 7:1 (based on the relative intensity of the ^{1}H/^{15}N peaks (Figure 1a) and so this peak is more reasonably assigned to the 3′G (G(8)), rather than the 5′G (G(7)) monofunctional adduct. At later time points the G(8) H8 peak for **3** is coincident with that of the G(18) H8 peak of the bifunctional adduct (**5**) (Figure 2a). Although no peak for the second 5′G monofunctional species is observed, it is also

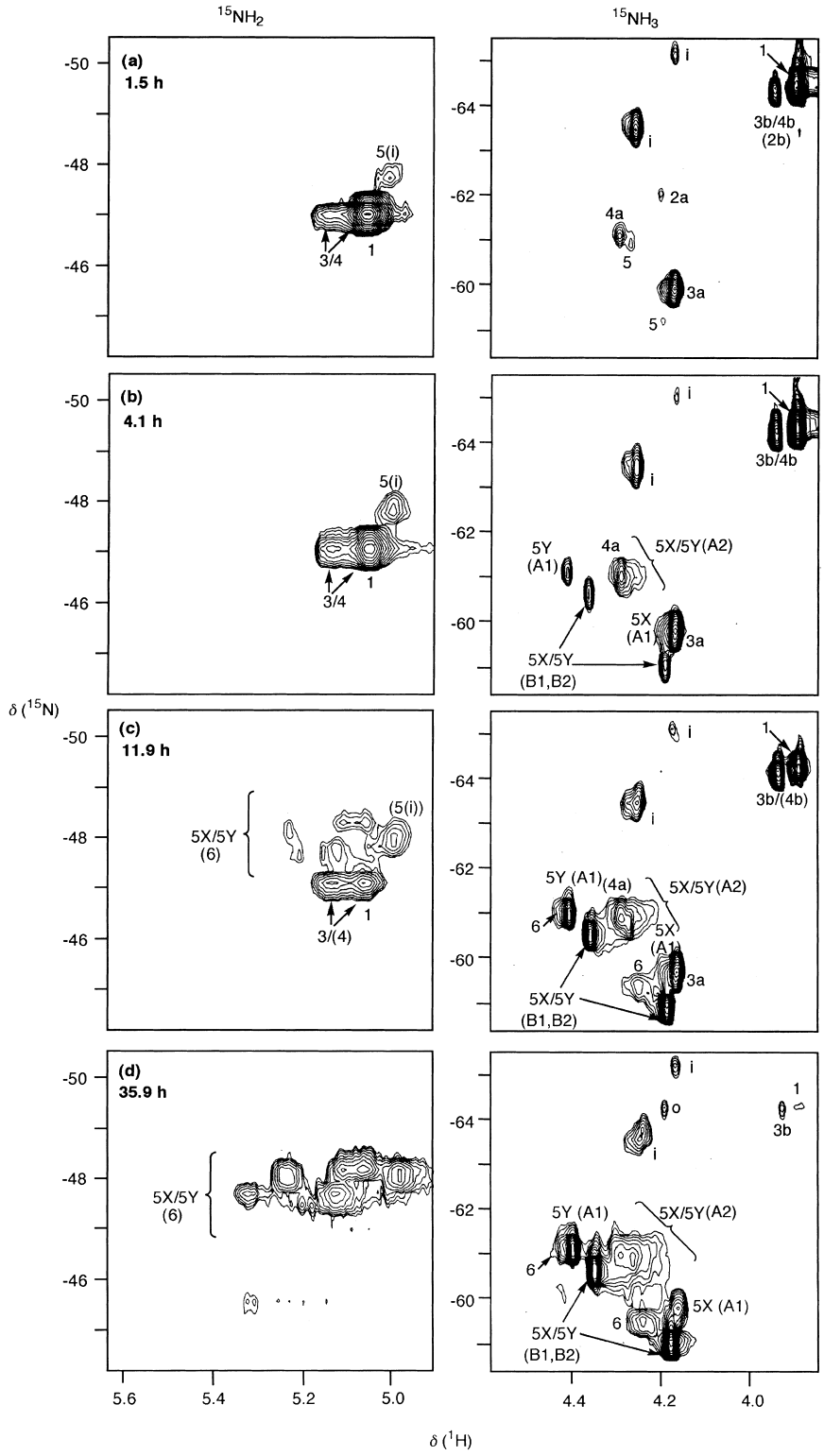

Figure 1. 2D [^{1}H,^{15}N]-HSQC NMR (600 MHz) spectra at 298 K of duplex **I** after reaction with ^{15}N-**1** for a) 1.5, b) 4.1, c) 11.9 and d) 35.9 h. Peaks are assigned to the NH_3 and NH_2 groups in structures **1**–**6** (see Scheme 1 and Table 1). Peaks labeled i and o are due to minor impurities in the sample of ^{15}N-**1**.[11] The major 3′G monofunctional adduct (**3**) converts into two conformers of the 1,4-(G(8)G(18)) interstrand adduct (**5X** and **5Y**). The assignments A_1/A_2 and B_1/B_2 correspond to the different NH_3 environments observed in the model (Supporting Information Figure S5), which are hydrogen bonded to O6 of the bases (B) and located close to the phosphate backbone (A). The minor peaks labeled **6** form more slowly and are tentatively assigned to the 1,4-(G(7)G(25)) interstrand adduct which forms from the minor 5′G monofunctional adduct (**4**). The peaks in the NH_2 region indicate that the Pt–NH_2 groups of both **5X** and **5Y** initially exist in similar solvent exposed environments (**5(i)**), but for the final product there are several different environments for the Pt–NH_2 groups.

likely to be obscured by the resonances of the G(8) or G(18) H8 protons of the bifunctional adduct, which achieves a greater concentration than the 5′G monofunctional adduct (G(7), **4**) after approximately 3 h (Figure 2a).

Other ^{1}H peaks are observed in the imino and thymine methyl regions with time dependent profiles consistent with the monofunctional adduct **3**.

Monofunctional binding of **1** and cisplatin to G(8) of the duplex **I** appear to induce similar localised distortions in the DNA structure based on 1) a strongly shielded T CH_3 resonance which is most reasonably assigned in both cases to T(9) (cisplatin, δ 1.214[13]; **3**, δ 1.122 (Figure 2c) and 2) a deshielded imino resonance, most likely corresponding to the T(9)·A(20)base-pair (cisplatin, δ 13.56[13]; **3**, δ 13.60 (Figure 2d).

Formation of the bifunctional adduct(s): ^{1}H,^{15}N peaks assignable to the 1,4-interstrand GG adduct (**5**) are visible after approximately 1.5 h. Closure of **3** to form a bifunctional cross-link could occur directly and/or involve prior aquation of **3** to form a G/H_2O intermediate. No peak assignable to an aquated monofunctional adduct, expected close to the peak for the {PtN_3O} group of the monoaqua monochloro species, was observed although it could be coincident with the peak for **2**, which disappears rapidly. In the Pt–$^{15}NH_3$ region the first sets of peaks assignable to the bifunctional adduct are broadened peaks centred at δ 4.27/–60.7 close to the 5′G (G(7)) monofunctional peak (**4a**), and two sharper peaks at δ 4.37/–60.4 and δ 4.20/–59.2 (just visible in Figure 1a). A further broadened peak (δ 4.18/–59.8) is overlapped with the 3′G (G(8)) monofunctional peak (**3a**) and is visible when the reaction is complete (Figure 1d). From the NOESY spectrum of the final product (Figure 3), the molecular models of the 1,4-interstrand cross-link,[21] and comparison with the [^{1}H,^{15}N]-HSQC NMR spectra from the analogous reaction with duplex **II**, [12] the spectrum can be interpreted as formation of one conformer of the 1,4 G(8)G(18) adduct **5**, referred henceforth as conformer **X**. The pair of peaks at δ 4.37/–60.4 and 4.20/–59.2 have an identical time dependence and are assigned to the Pt–NH_3 environments B_1

0947-6539/03/0903-0716 $ 20.00+.50/0 *Chem. Eur. J.* **2003**, *9*, No. 3

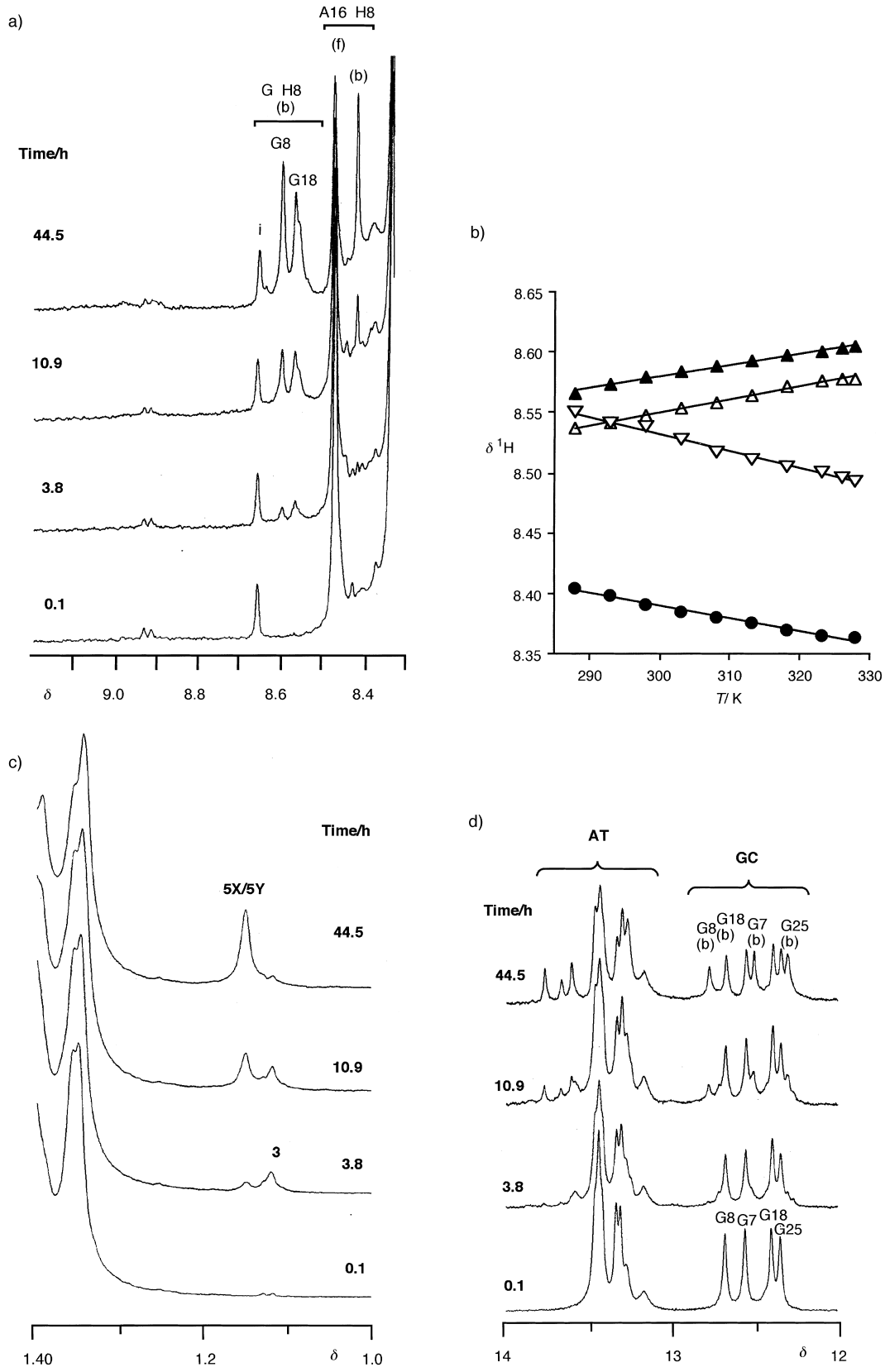

Figure 2. Selected regions of the ^{1}H NMR spectra (600 MHz) of duplex **I** after reaction with ^{15}N-**1** for between 0 and 45 h. In a) the peaks are assigned (from the NOESY spectrum) to the H8 resonances of the A16 (f, free, b, bound) and G(8) and G(18) bases coordinated to platinum in the 1,4-interstrand cross-link (**5**). There are two distinct G(18) H8 resonances attributable to the two conformers **5X** and **5Y** which are almost superimposed at 298 K. The temperature dependence of the chemical shifts of these resonances is shown in b):▲ G(8) H8, △ and ▽ G(18) (H8), ● A16 H8. In c) shielded thymine methyl resonances occur for the 3′G monofunctional adduct (**3**, T(9)) and the two conformers of the 1,4G(8)(G(18) cross-link (**5X**, **5Y**, T(17)). In d) the assignments of resonances to the G H1 and T H3 imino protons in the free duplex are from ref. [17] and those at 45 h are from the NOESY spectrum. Although the reaction is complete at 45 h signals for unplatinated **I** are present due to the excess of DNA used in the reaction.

  0947-6539/03/0903-0717 $ 20.00+.50/0

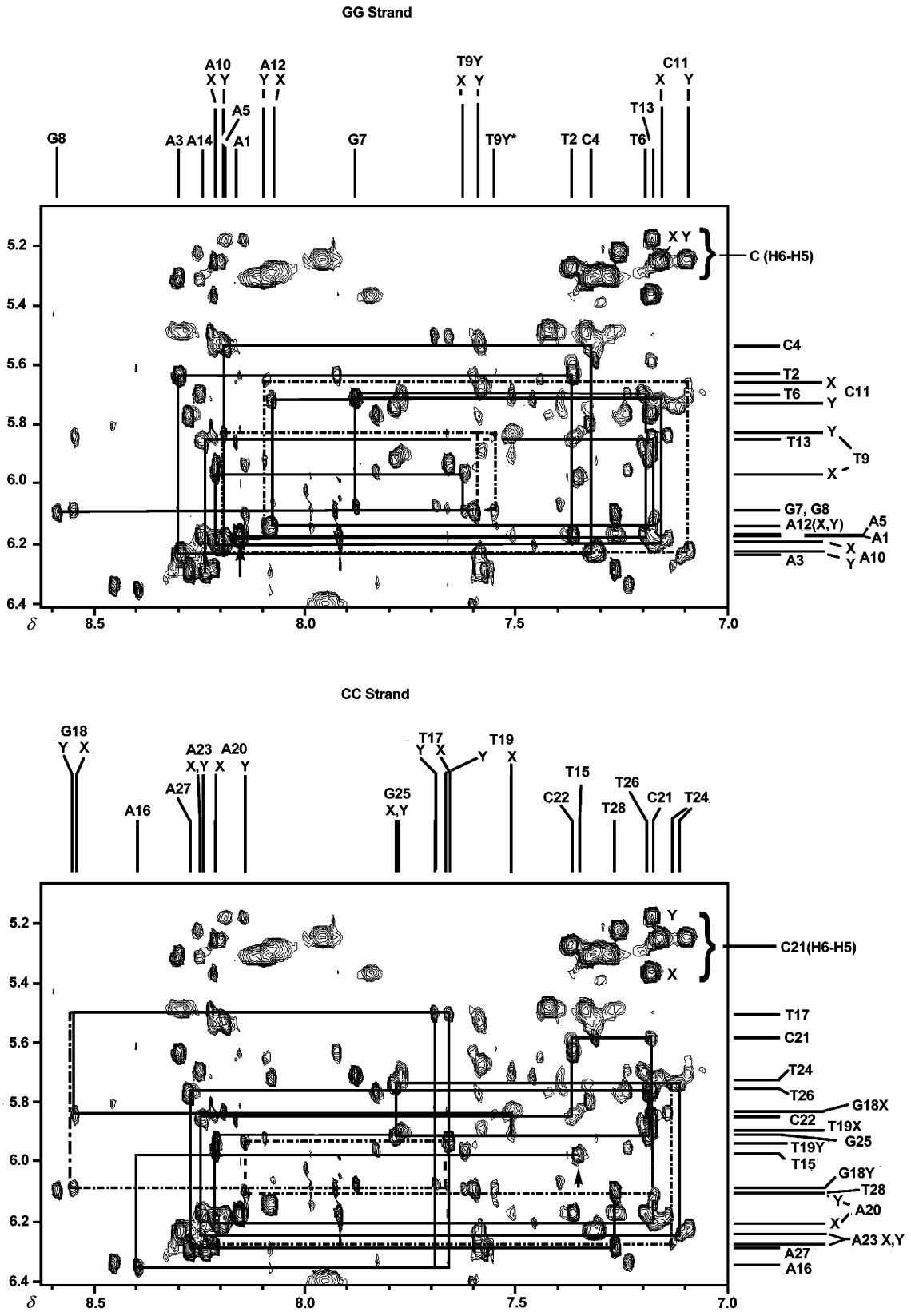

Figure 3. NOESY NMR spectra (600 MHz, 298 K) of the final product of the reaction between **1** and **I**. The duplicate contour plots show the aromatic to sugar ring H1′ connectivities. The sequential NOESY assignment walks are shown in a) for the GG strand and b) for the complementary CC strand of the platinated adduct. The sample (different to that in Figures 1 and 2) contains a slight excess of unreacted duplex **I** and the equivalent assignments pathways for these sets of cross-peaks were made with reference to the published data[17] and are shown in the Supporting Information (Figure S3). The plots show two assignment pathways consistent with two conformers of the 5′–5′-G(8)G(18) inter-strand cross-link. Connectivities for the major conformer (**X**, solid line) and minor conformer (**Y**, dashed line) are on the basis of connectivities to the C(11) and C(21) H6 protons and the relative volumes of the C H6 to H5 cross-peaks. For T(9) there are two possible assignments for the H6 proton of the minor conformer **Y** (see Table S2 in Supporting Information).

0947-6539/03/0903-0718 $ 20.00+.50/0 *Chem. Eur. J.* **2003**, *9*, No. 3

and B_2, which are coordinated to different Pt atoms and (in the model) are both hydrogen-bonded to a guanine O6. The broader peaks close to peaks **4a** and **3a** are assigned to the Pt–NH_3 A_1 and A_2 environments. In the model[21] these groups point out of the major groove, towards the phosphate oxygen atoms of the DNA backbone (see below).

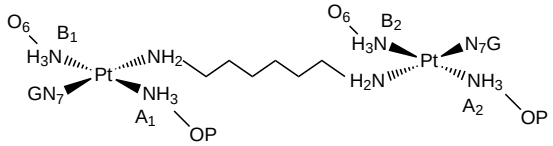

These assignments also follow those elucidated for the analogous conformers formed in the reaction of ^{15}N-**1** with duplex **II**,[12] the major difference being that in the previous case, there was only one peak (δ 4.39/ – 60.5) assignable to both B_1 and B_2 environments. This difference is consistent with the self-complementary (**II**) versus the palindromic (**I**) nature of the two sequences.

A new strongly deshielded sharp peak at δ 4.42/ – 60.9 is first visible after about 2.5 h. This peak increases in intensity at approximately the same rate as the pair of peaks at δ 4.37/ – 60.4 and 4.20/ – 59.2. It shows an approximately equal volume to that of a new broadened peak that is coincident with the 5′G monofunctional peak **4a** (δ 4.30/ – 61.0) and is visible when the reaction is complete (Figure 1d). Based on the time dependence and relative intensities of all the Pt–NH_3 peaks assignable to the bifunctional adduct, these peaks are assignable to the Pt–NH_3 A_1 and A_2 of a second conformer (termed **5Y**). The B_1 and B_2 groups of **5Y** are assumed to be indistinguishable from those of **5X** and therefore contribute to the same two peaks at δ 4.37/ – 60.4 and 4.20/ – 59.2. The time dependence plots of the Pt–NH_3 peaks are provided in the Supporting Information. Based on the relative peak volumes at the end of the reaction the relative concentration of **5Y** : **5X** is about 1.2:1.0 or essentially 1:1 (see below).

In the Pt–$^{15}NH_2$ region the peaks assignable to **5** were first visible at the same time as peaks appeared in the NH_3 region (approximately 1 h after the start of the reaction). Initially, there was only one broadened peak at δ 5.00/ – 47.9 (labeled **5(i)** in Figure 1), which increased steadily in intensity for the first 6 h. The relative intensity then remained constant with the appearance of several new peaks with ^{15}N shifts in a narrow range centered at δ ^{15}N – 47.8 to – 48.3 (Figure 1 and Table 2). Individual Pt–NH_2 peaks for the **5X** and **5Y** conformers are not discernable.

In the aromatic region of the ^{1}H spectrum there are three major resonances attributable to the H8 protons of the coordinated G residues (Figure 2a). These were assigned (from the NOESY spectrum, Figure 3) to G(8) (δ 8.58) and G(18) (δ 8.55 and 8.54). At 298 K the two G(18) H8 resonances are almost superimposed but the peaks shift in opposite directions on changing temperature (Figure 2b) and above 298 K they are clearly resolved as separate peaks. The opposing temperature dependencies (+1.08 and -1.41×10^{-3} ppm K^{-1}) are consistent with different environments for the G(18) H8 protons in two different conformers. The two peaks have similar integrals, again indicating a ratio of approximately 1:1 for **5X** and **5Y**, consistent with the [^{1}H,^{15}N]-HSQC NMR data.

Table 2. ^{1}H and ^{15}N shifts for 1,4 GG interstrand adducts formed in the reaction of **1** with the duplex 5′-d(ATACATG(7)G(8)TACATA)·3′-d(TATG(25)TACCATG(18)TAT) (**I**) at pH 5.4, 298 K.[a]

Species	Label	Pt–NH_3		Pt–NH_2
1,1,t,t(n = 6)		δ ^{1}H	δ ^{15}N	δ ^{1}H/δ ^{15}N[f]
Y = N7G(8),	**5X**	4.20[b]	– 59.2	
Y′ = N7G(18)		4.37[b]	– 60.4	5.00/ – 47.9(24%)
		4.24 – 4.29[c]	ca – 61	5.15/ – 47.8 (22%)
		ca 4.18[c]	– 59.8	5.12 – 48.3 (15%)
	5Y	4.20[b]	– 59.1	5.08 – 48.2 (17%)
		4.37[e]	– 60.4	5.25/ – 47.9 (14%)
		4.42[d]	– 60.9	5.34 – 47.8 (4%)
		4.24 – 4.29[c]	ca – 61	5.20 – 47.5 (2%)
				5.09 – 47.7 (2%)
Y = N7G(7)	**6**[e]	4.44	– 61.2	[g]
Y′ = N7G(25)		4.26	– 59.6	
		4.24	– 59.3	

[a] ^{1}H referenced to TSP, ^{15}N referenced to $^{15}NH_4Cl$ (external), δ in ^{15}N dimension ± 0.2 ppm. [b] Sharp peak assigned to Pt–NH_3 groups (B_1/B_2) of **5X** and **5Y** hydrogen bonded to G O6 groups. [c] Broad series of peaks assignable to the Pt–NH_3 groups of **5X** (A_1/A_2) and **5Y** (A_2) close to the phosphate backbone. [d] Sharp peak assigned to Pt–NH_3 group (A_1) of **5Y** hydrogen bonded to phosphate. [e] Tentative assignment (see text); an additional peak is assumed to be obscured by the broad peaks for the A_1/A_2 Pt–NH_3 groups of **5X** and/or **5Y**. [f] The peak at 5.00/ – 47.9 appears first (ca. 1 h), and the other peaks become visible after *ca* 6 h (Figure 1); individual peaks for **5X** and **5Y** can not be distinguished; the % contribution of each peak to the final product is shown in parentheses. [g] Cannot be distinguished from the peaks for **5**.

Minor Products: Further new peaks in the Pt–NH_3 region appear more slowly and are first visible after about 6 h (Figure 1c). Two peaks with equal intensity and similar ^{1}H/^{15}N shifts (δ 4.26/ – 59.6 and 4.24/ – 59.3) have similar intensity and time dependent profiles to a shoulder of the **5Y** Pt–NH_3 A_1 peak (δ 4.42/ – 60.9). It is assumed that the peaks correspond to a product other than the G(8)G(18) adduct and a tentative assignment is a 1,4 G(7)G(25) cross-link (**6**) that could form from the minor 5′G (G(7)) monofunctional adduct. In parallel studies to form site-specific oligonucleotide adducts, the formation of these 3′–3′-interstrand cross-links have in fact been observed with the trinuclear complex BBR3464.[22] It is assumed that the three peaks correspond to three of the NH_3 groups of the adduct and a fourth peak is overlapped with the broad peak(s) for the Pt–NH_3 A groups of **5X** and **5Y**. The total peaks for **6** account for about 10% of the total product. Although in the Pt–NH_2 region, peaks for the different product species are not discernable, there are minor peaks with relative intensity consistent with the minor product **6** (see Table 2). Three minor peaks (δ 8.63, 8.53, and 8.50) observed free from overlap in the ^{1}H spectrum at 328 K are possibly assignable to GH8 protons in the minor adduct. One of these peaks is visible (at δ 8.63) in the spectrum at 298 K (Figure 2a).

Characterization of the bifunctional adduct: A 2D NOESY NMR spectrum of the final product from the reaction between **1** and duplex **I** was collected at 298 K, on a sample that contained a slight excess of unreacted duplex. Although

the complexity of the spectrum precluded measurement of an extensive set of NOEs, the analysis enabled the unambiguous characterization of the major adduct, as well as providing some structural information. Correlations between the aromatic and sugar H1′ protons are shown in Figure 3. The ^{1}H resonances of unmodified **I** were readily assignable in this region by reference to the published data.[17] Complete sets of sequential connectivities between *n*H8/H6 to *n*H1′ and between *n*H1′ to $(n+1)$H8/H6 were traced for the separate strands of duplex **I** (see Figure S3 in Supporting Information), and from these assignments it was possible to trace the equivalent assignment pathways for the two conformers of the major platinated adduct. Where cross-peaks were either missing or obscured by overlap, the aromatic proton assignments were confirmed from connectivities to the sugar H2′/H2″ protons and/or connectivities between thymine $n(CH_3)$ and G or A $(n-1)$H8 protons. The chemical shifts for the aromatic, H1′ and thymine CH_3 protons are given in the Supporting Information (Table S2) and changes in chemical shift of the aromatic base resonances are shown pictorially in Figure 4. It is apparent that the largest chemical shift changes between the unmodified and platinated duplex occur for the G(8) ($\Delta\delta$ 1.01 ppm) and G(18) ($\Delta\delta$ 0.72 ppm) H8 resonances, consistent with the binding Pt to N7 of these bases. There are also significant changes in chemical shift for aromatic protons of the bases adjacent to the platinated residues. However, no significant change (<0.02 ppm) for the five base-pairs at the 5′ end of the sequence is observed, indicating that the G(25) base is not platinated in the major adduct.

At the temperature at which the NOESY spectrum was recorded (298 K), there is a chemical shift difference of 0.02 ppm between the resonances for the G(18) H8 protons in the two conformers **5X** and **5Y** (Figure 2b). Although in both cases cross peaks between G(18) H8 and T(17) H1′ and T(17) H6, and A(16) H1′ were missing (Figure 3), it was nevertheless possible to trace the sequential connectivities for the two conformers. For the aromatic protons (Figure 4a) the chemical shift changes in each case are very similar, with the

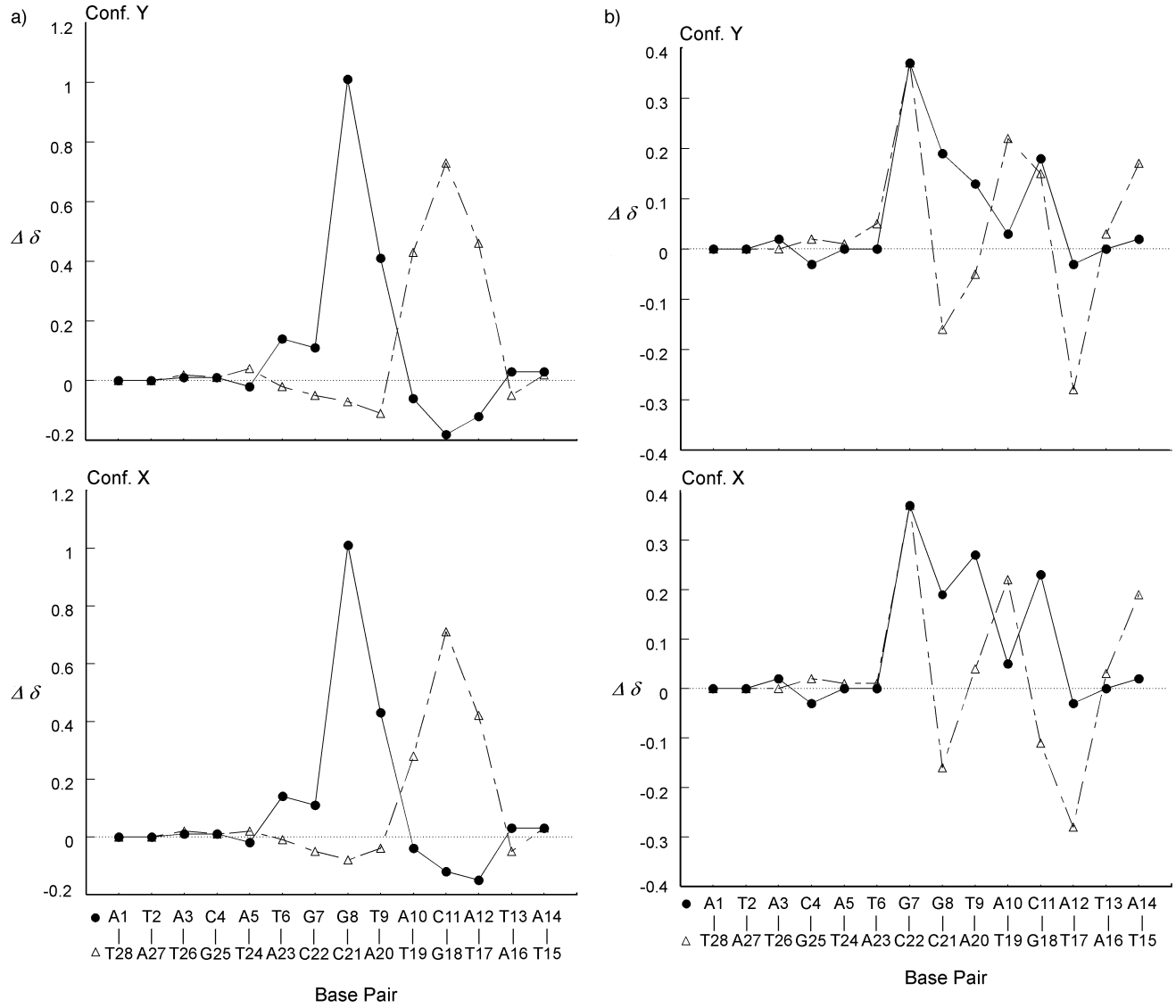

Figure 4. Changes in the chemical shifts ($\Delta\delta$, ppm) of a) the aromatic protons of the two strands of duplex **I** and b) the sugar H1′ protons, on formation of the bifunctional adduct with **1**. (labels: **Ia** (● solid lines), **Ib** (△, dashed lines)). The chemical shifts for the aromatic, H1′, and thymine CH_3 protons for free duplex and bifunctional adduct are given in the Supporting Information (Table S2).

0947-6539/03/0903-0720 $ 20.00+.50/0 *Chem. Eur. J.* **2003**, *9*, No. 3

notable exception of protons on bases close to the platinated G(18) residue (T(19) H6, and to a lesser extent A(20) H8, and C(11) H6, indicative of some structural differences for the two conformers in this region.

The profiles for the shifts of the H1′ protons in the two conformers are also similar (Figure 4b) with the notable exception again of G(18), A(20), C(11), and T(9). It is interesting that for the platinated bases (G(8) and G(18)) the magnitude of the changes in H1′ shifts are quite similar ($\Delta\delta =$ 0.11 – 0.19 ppm), as are those of the complementary bases C(21) and C(11) ($\Delta\delta = 0.16 - 0.23$ ppm), (ignoring sign in both cases), but the largest changes ($\Delta\delta = 0.28 - 0.37$ ppm), are for the bases 5′ to the platinated G on each strand (e.g. G(7) and T(17)). Structural changes are evident for bases up to three base-pairs from the platination sites. The results are in stark contrast to those of the cisplatin-adduct of this sequence, for which significant changes in H1′ shift are found only for the platinated G(7),G(8) bases, and T(6).[17] The results are also very similar to the chemical shifts found for the 1,4-interstrand cross-link formed by BBR3464 in the 8-mer duplex (5′-ATGTACAT-3′)$_2$.[23] Unpublished results indicate a very similar structure for the adduct formed by the dinuclear **1** with this latter sequence.[24] In these cases, the T 3′ to the Pt-G (analogous to T(9) and T(19) in this case) suffers a large 0.45 ppm shift and the T analogous to T(17) also suffers a significant shift. Monofunctional binding to guanines tend to produce high *anti* or *syn* conformational changes in the nucleotide backbone. The interstrand cross-linking sequence -GTAC- is identical in both cases (the 8-mer and the 14-mer here) and thus immediate local conformational changes are likely to be very similar. Strong H8/H1′ intraresidue cross-peaks for the A(12) and A(16) residues, weak or absent A(12)H1′/T(13)H6, and A(16) H1′/T(17)H6 cross-peaks (Figure 3) are similar to those observed for the analogous bases (A7 and A1) in the shorter 8-mer sequence, and are again consistent with an unusual *syn*-conformation for adenine bases not directly involved in the cross-link.

Kinetic analysis: The reaction between ^{15}N-**1** and duplex **I** was subjected to kinetic analysis. The treatment of the [^{1}H,^{15}N]-HSQC NMR peaks in the Pt–$^{15}NH_3$ region and the estimated concentration of each species for each spectrum is provided in detail in the Supporting Information. Due to peak overlap the total monfunctional and total product species can be determined accurately; however, the concentration of the individual species is obtained after correcting for the overlap (see Supporting Information). For this reason, the kinetic data was fitted to three models in which the monofunctional species (**3** and **4**) and product species (**5** and **6**) were either treated separately or summed together. The reaction pathway for Model 1 (which considers all species separately) is shown in Scheme 3, and full details of the three kinetic models are provided as Supporting Information. The pre-covalent binding association of **1** and **2** with the duplex was not considered and both species were treated as unbound. The aquation step was modeled as an irreversible pseudo-first-order process. The aquation of **1** occurs such that the equilibrium between aquated and chloro species lies strongly towards the chloro side, and is reflected by a large value for the anation rate constant.[11] In the presence of duplex **I** this equilibrium is removed as, once formed, the aqua chloro species **2** reacts rapidly and irreversibly with the duplex. Binding of **2** to the duplex **I** was treated as an irreversible second-order reaction, first-order with respect to the concentration of both **2** and **I**, respectively. Since no ^{1}H/^{15}N peak was observed assignable to a monofunctional aqua species, the formation of the bifunctional cross-links (**5** and **6**) were modeled to be formed directly from the monofunctional adducts. Both processes were treated as irreversible first-order reactions with respect to the concentration of **3** or **4**. The rate constants obtained from kinetic Model 1 (Scheme 3) are listed in Table 3 and the computer best fits for the rate constants are shown in Figure 5. A comparison of the rate constants obtained from the three kinetic models is provided as Supporting Information.

Table 3. Rate constants for the reaction of **1** with duplex **I** at 298 K, (pH 5 4).[a]

Rate constant	Model 1
k_H [10^{-5} s^{-1}]	4.00 ± 0.03
$k_{3'}$ [M^{-1}s^{-1}]	1.5 ± 0.7
$k_{5'}$ [M^{-1}s^{-1}]	0.24 ± 0.11
$k_{3'C}$ [10^{-5}s^{-1}]	4.47 ± 0.06
$k_{5'C}$ [10^{-}s^{-1}]	2.7 ± 0.2

[a] The NMR data were analyzed by three different kinetic models, as described in the text. The preferred model, Model 1, is shown in Scheme 3 and the computer best fits to the rate constants are shown in Figure 5. The errors represent one standard deviation. Full details of the three kinetic models and the rate constants obtained from Models 2 and 3 are provided in the Supporting Information.

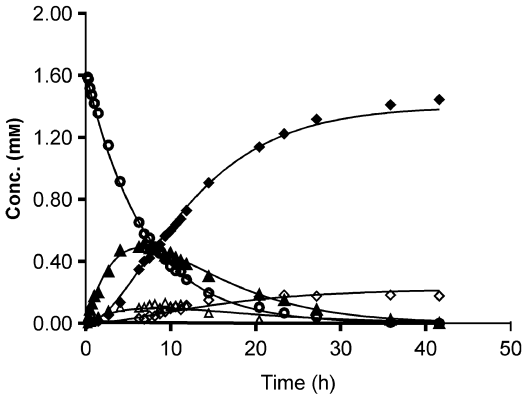

Figure 5. Plot of the relative concentration of species observed during the reaction at 298 K between **I** and ^{15}N-**1** based on Model 1 (Scheme 3). The concentrations are based on the relative peak volumes of peaks in the Pt–NH_3 region. The curves are computer best fits for the rate constants shown in Table 3. (labels: **1** O open circles, **2** asterixes, **3** closed triangles, **4** open triangles, **5** closed diamonds, and **6** open diamonds).

The pseudo-first-order rate constant for the aquation of **1** is the same for all three kinetic models and is similar to the value obtained for the reaction of **1** with the 12-mer duplex **II** ($4.15 \pm 0.04 \times 10^{-5}$ s^{-1}).[12] The rate constant for monofunctional binding is similar in all three models; the large error associated with $k_{3'}$ is primarily a consequence of the dearth and scatter of data for the concentration of the aquachloro

species **2**. Monofunctional adduct formation to the 3′G is significantly faster than observed for binding of **1** to the isolated guanine base on duplex **II** (rate constant $\sim 0.47 \pm 0.07\,\text{M}^{-1}\,\text{s}^{-1}$).[12] The fact that so little of the aquachloro species **2** is seen in the reaction with **I**, relative to the amounts observed with duplex **II**,[12] is consistent with a more rapid reaction with the duplex **I**, preventing the build up of its concentration.

The rate constants associated with conversion of monofunctional adducts to bifunctional adducts are slightly higher but with a similar order of magnitude to the formation of the 1,4-interstrand cross-link on duplex **II** ($3.39 \pm 0.04 \times 10^{-5}\,\text{s}^{-1}$).[12] In both cases the cross-links span the same number of bases and for the G(8)–G(18) cross-link, these bases are identical to those for the duplex **II.**

The overall reaction is complete within 40 h, which is slightly faster than that observed in the reaction between **1** and duplex **II** (48 h).[12] This is due to higher rate constants for both monofunctional and bifunctional binding. The overall rate-determining step remains the aquation of **1**, which is similar for both reactions.

Discussion

The binding of **1** to the DNA duplex **I** follows the general outline previously delineated for similar sequences. As for the reaction between **1** and the self-complementary 12-mer duplex 5′-{d(ATATGTACATAT)$_2$} (**II**),[12] there is clear evidence for preassociation of the drug with the DNA, prior to aquation and covalent binding. This is seen from both the shift in the position of the ^{1}H/^{15}N peaks for the a(m)mine groups of **1** and also by shifts in certain ^{1}H resonances of the DNA (see below). In contrast to the self-complementary sequence **II** in the previous study,[12] duplex **I** is palindromic. This difference is reflected in the unsymmetrical shape of the ^{1}H/^{15}N peak for preassociated **1**, indicating that the NH_3 groups on the two Pt atoms are interacting with non equivalent environments on the duplex.

The pseudo-first-order aquation rate constant of **1** in the presence of **I** is more than twofold greater than that for cisplatin with the same sequence under similar conditions (298 K, pH 6.0).[13] This result is expected because the aquation (and anation) of complexes of the general form {$PtClN_3$} have been shown to be more rapid than for those of complexes of the form {$PtCl_2N_2$}, with equilibrium conditions achieved far more rapidly, and the position of the equilibrium lying strongly towards the chloro form.[11]

As observed for the reaction with the duplex **II**,[12] the aquation of **1** appears to be slowed relative to that observed in the absence of DNA.[11] This retardation could be a consequence of limiting solvent access to the Pt center through the observed electrostatic interaction between the dipositive **1** and the polyanionic DNA. The suggestion that pre-association of the platinum centers with duplex DNA could hinder formation of the five-membered transition state necessary for substitution (aquation) reactions, is supported further from recent new evidence that shows the aquation of **1** to be faster by a factor of 1.4 in the presence of the single strand **Ia**, compared to duplex **I**, under identical conditions.[25]

Our results show formation of one major monofuctional adduct on reaction of **1** with duplex **I**, and we can conclude that binding to the 3′G (G(8)) is at least sixfold faster than binding to the 5′G (Table 3). Similarly, the 3′G is preferred when cisplatin binds to the same sequence, with binding to G(8) about fourfold faster than to G(7) (for both single-strand **Ia** and duplex **I**).[13, 18] More rapid binding to the 3′ base of an intrastrand purine-purine grouping has also been observed with different sequences.[26] Monofunctional binding of **1** to **I** is approximately threefold faster than binding to the isolated guanine in the 12-mer 1,4 sequence **II**,[12] a result of the enhanced nucleophilicity associated with the GG binding site relative to isolated guanine residues.[27] Further, binding to the 3′G of **I** is about threefold faster for **1** (aquated form) than for *cis*-[$PtCl(OH_2)(NH_3)_2$] ($0.47 \pm 0.08\,\text{M}^{-1}\text{s}^{-1}$).[13]

Previous DNA binding studies using molecular biology techniques have revealed that the dinuclear compound **1** forms predominantly interstrand cross-links in the 5′–5′ direction.[16, 28–30] The results of this competition experiment are consistent with this trend with formation of only one major adduct, shown conclusively, by analysis of the NOESY spectrum, to be the 1,4-G(8)G(18) interstrand cross-link. The 5′–5′ specificity can be rationalized, first of all by the preference for initial monofunctional binding at the 3′-G of the GG site and the inability of the linker group to span five base pairs (eliminating the possibility of the 3′–3′ 1,5-G(8)(G25) adduct). Secondly, the molecular model of the monofunctional adduct (Supporting Information, Figure S4) shows an electrostatic interaction between the unbound {PtN_3Cl} end group and the DNA, consistent with the ^{1}H shift of this $Pt(NH_3)_2$ group, which is significantly deshielded with respect to the ^{1}H/^{15}N peak of unbound **1** (Figure 1). The proximity of the {PtN_3Cl} group to the G(18) base in the molecular model indicates that initial monofunctional binding at G(8) would promote preferential closure to the 5′–5′ 1,4-interstrand cross-link. An intriguing possibility could suggest prior recognition of the 1,4 G(8)G(18) interstrand binding site in the initial preassociation of **1** with the DNA. The initial ^{1}H NMR spectrum of **I** in the presence of **1** shows that the pre-association induces shifts in the resonances corresponding to protons on the adenine residues of the base pairs flanking the G(18) binding site, (A(10) H2 and H8, A(12) H8).

The clinical drug BBR3464 produces a smaller percentage of interstrand cross-links than **1** and footprinting studies indicate the formation of cross-links in both the 5′–5′ and 3′–3′ directions.[22] It is of interest to determine whether pre-association affects the directional nature as well as the extent of the interstrand cross-links. In preliminary experiments we have investigated the reaction of BBR3464 with duplex **I** and ^{1}H NMR studies show that pre-association of the drug with the DNA selectively perturbs the imino resonances of three of the four GC base pairs (G(18).C(11), G(25)·C(4), and G(7)·C(22)).[31] Further studies are in progress to characterize the products of the reaction and will reveal whether this preassociation influences the formation of 5′–5′ ((G(8/7)-G(18)) versus 3′–3′ ((G8/7)G(25)) adducts. In other [^{1}H,^{15}N]-HSQC NMR studies we have followed the formation of 1,4-

0947-6539/03/0903-0722 $ 20.00+.50/0 *Chem. Eur. J.* **2003**, *9*, No. 3

and 1,6-GG interstrand cross-links by reaction of ^{15}N-BBR3464 with the self-complementary sequences 5′-d(ATATGTACATAT)-3′ and 5′-d(TATGTATACATA)-3′[31] Analysis of the [^{1}H,^{15}N]-HSQC and ^{1}H NMR spectra reveal that strong and directed preassociation of the charged $\{PtN_4\}^{+}$ linker group in the minor groove has a profound influence on the structures of the interstrand cross-links that form for the two sequences.

In the present study, our data alone can not exclude the possibility that the minor product (**6**) observed in the [^{1}H,^{15}N]-HSQC NMR spectra is the 1,2-G(7)G(8) intrastrand cross-link. However, even if this is the case it represents only about 10% of the total product. A more likely assignment for **6** is the 3′–3′ 1,4-G(7)(G25) adduct, which would be the expected product to form from the minor 5′-G monofunctional adduct. Molecular mechanics studies indicate that the 1,4-interstrand cross-link is energetically preferred over the 1,2-intrastrand cross-link.[32]

Overall, this work has further demonstrated the utility of the [^{1}H,^{15}N]-HSQC NMR method in probing Pt-drug–DNA interactions and in obtaining detailed information on interactions at the molecular level that can not be obtained by other methods. It is notable that analysis of the [^{1}H,^{15}N]-HSQC NMR spectra (in conjunction with the ^{1}H NMR spectra) indicated that there were two conformational forms of one major bifunctional adduct, which was predicted to be the 1,4-G(8)G(18) cross-link. This prediction was subsequently confirmed from the assignment of the NOESY spectrum of the final product, but the complexity of this spectrum would have precluded assignment of the sequential connectivities without prior knowledge that the cross-peaks were derived from an approximate 1:1 mixture of two independent conformers (plus a small amount of unreacted duplex **I**). Consideration of the ^{1}H/^{15}N shifts of the Pt–NH_3 groups in the bifunctional adduct(s) allowed us to speculate that the major difference between the two conformers is that for one (**5Y**) there is a strong hydrogen-bond between one Pt–NH_3 group (A_1) and the phosphate backbone which is not present for the equivalent Pt–NH_3 group in the second conformer (**5X**). These differences are seen in the molecular models of the two conformers of the G(8)G(18) interstrand cross-link.[21]

Changes in the shifts of aromatic and sugar H1′ protons show that there are significant structural changes in the DNA, even for bases some distance apart from the platination sites. These structural changes are propagated along the duplex beyond the localized influence of the drug in the direction (A(12)–A(14)), but not in the other (T(6)–A(1)) (see Figure 4b). The NMR structure of the 1,4-interstrand cross-link formed by BBR3464 with the self-complementary alternating purine–pyrimidine 8-mer 5′-$(ATGTACAT)_2$ also shows delocalized distortions beyond the binding site, specifically the induction of the *syn* conformation on the adenines.[23]

Also, changes in H1′ shift are propagated along the alternating purine–pyrmidine region of the sequence G(8)·C(21) to A(14)·T(15) and stop where the sequence is broken at G(7)–C(22). Both di- and trinuclear Pt compounds of this class induce an irreversible B → Z conformational change in poly(dG-dC)·poly(dG-dC).[33] A strict structural requirement for the left-handed Z conformation is alternating purine–pyrimidine sequences. In the present case, the major changes are also propagated in the alternating purine–pyrimidine motif, leading to the possible creation of B/Z junctions, in this case at the G(7)G(8) step. This also explains the apparent lack of distortion whereby the B-form of the DNA is conformationally restrictive.

Chemical probes have been used recently to study structural perturbations of 1,4-interstrand GG cross-links of BBR3464 oriented in both 5′–5′ and 3′–3′ directions.[22] Within the sequence (5′-…TCAT$^{\#}$T$^{\#}$G*TTCTTCC…-3′)–(5′-…GGAAG*AACA$^{\#}$A$^{\#}$TA…-3′′), in which G* represents the platination site, treatment with $KMnO_4$ revealed strong perturbation for the two 5′T residues (marked T$^{\#}$) adjacent to the adduct. For the 5′–5′ 1,4-interstrand G(8)–G(18) cross-link of **1**, the equivalent 5′T residue is T(17). For both conformers the T(17) residue is strongly perturbed as shown by 1) a strongly shielded CH_3 resonance ($\delta\Delta$ –0.30 ppm, Figure 2c), 2) no inter-residue thymine $n(CH_3)$/A $(n-1)$H8 cross-peak and 3) unusually strong intra-residue cross-peaks between T(17) H6 and H5′/H5′′(or H4′) sugar protons. The NMR data also indicate a *syn* conformation for the complementary adenine A(12) which helps explain the observed chemical probe reactivity for similar sequences.

Conclusion

We have shown from competition experiments that the dinuclear platinum complex **1** preferentially forms a 1,4-interstrand GG adduct orientated in the 5′–5′ direction on binding to the 14-mer duplex **I**. A minor product (<10%) is likely to be the 3′–3′ 1,4-interstrand GG cross-link and not the 1,2-GG intrastrand adduct. Pre-association of the drug with the DNA could play a role in the 5′–5′ specificity as there is some evidence for prior recognition of the 1,4-interstrand cross-link in the pre-associated complex. The specificity is also attributable to more rapid binding to the 3′G of the -GG- binding site and the inability of **1** to span more than five base pairs. The overall formation of the 1,4-interstrand cross-link is faster than observed for the self-complementary 12-mer sequence **II**, largely a consequence of more rapid monofunctional binding due to the enhanced nucleophilicity associated with the GG binding site relative to an isolated guanine residue. From these results we can predict that 1,4-interstrand 5′–5′ cross-links located at -GG- binding sites are likely to be major lesions for **1** and related polynuclear complexes that can span four base pairs. There are two conformational forms of the 1,4-interstrand cross-link that differ in the orientation of the platinum coordination plane in relation to the plane of the bound G(18) residue. For both conformers structural changes are propagated along the duplex beyond the localized influence of the drug. There is evidence for *syn* conformations of adenine bases not directly involved in the cross-link, as also seen for a 1,4-interstrand cross-link of BBR3464 with a shorter -GTAC- sequence. A significant distortion of the 5′T residue adjacent to the adduct is consistent with the results of other studies that have used chemical probes to analyse the DNA

  0947-6539/03/0903-0723 $ 20.00+.50/0

conformation of 1,4-interstrand cross-links formed by BBR3464.

Experimental Section

Materials and sample preparation: The sodium acetate salts of HPLC purified oligonucleotides were purchased from OSWEL. The nitrate salt of $[\{trans\text{-}Pt Cl(^{15}NH_3)_2\}_2(\mu\text{-}H_2{}^{15}N(CH_2)_6{}^{15}NH_2)]^{2+}$ (fully ^{15}N-labeled 1,1/t,t (**1**)) was prepared as described elsewhere.[11]

Preparation of DNA duplex (I): Stock solutions of 5′-d(ATACATGGTACATA)-3′ (**Ia**) and 5′-d(TATGTACCATGTAT)-3′ (**Ib**) were prepared in 500 μL of 5% D_2O in H_2O. The concentrations were estimated spectrophotometrically to be 16.9 mmol and 20.8 mmol, respectively using the absorption coefficients ($\varepsilon_{260} = 110.3 \times 10^3\,M^{-1}cm^{-1}$ (**Ia**) and $101.4 \times 103\,M^{-1}cm^{-1}$ (**Ib**)), calculated using the method of Kallansrud and Ward.[34]

Platination of duplex I by ^{15}N-1: Duplicate reactions were carried out as follows: Stock solutions of **Ia** (63.8 μL of 16.9 mm solution in 5% D_2O/95% H_2O, 1.08×10^{-6} mol), and **Ib** stock solution (53.9 μL of 20.8 mm solution in 5% D_2O/95% H_2O, 1.12×10^{-6} M, 1.04 equiv.), sodium phosphate buffer solution (30 μL, 200 mM, pH 5.3), TSP (sodium 3-trimethylsilyl-[D_4]-propionate) (2 μL, 13.3 mM) and 5% D_2O in H_2O (230.3 μL) were combined into a 5 mm Shigemi NMR tube, and the pH was measured (5.3–5.4). A volume of 5 μL was used for the pH measurement giving a reaction mixture of volume 375 μL containing duplex **I** (1.06×10^{-6} M). A melting profile was carried out on the unplatinated duplex **I** by obtaining ^{1}H spectra at 5 K increments between 298 K and 326 K. After allowing the solution to slowly cool back to 298 K an aliquot of a freshly prepared chilled solution of ^{15}N-**1** (20 μL 1.11 mg, 1.43 μmol) in 5% D_2O in H_2O (44.7 μL) was added to give reactant and buffer concentrations of (**I**) (2.69 mM), phosphate buffer (15 mM) and ^{15}N-**1** (1.62 mM). The reactions at 298 K were followed by a series of ^{1}H and [^{1}H,^{15}N]-HSQC NMR spectra over the period of 0–41.5 h.

Characterization of the platinated adduct: To characterise the final product by analysis of the NOESY spectrum, the reaction was repeated with the ratio of **1** to **I** closer to unity to avoid the large excess of unreacted **I**. The NMR tube contained the following: TSP (2 μL, 13.3 mM in 5% D_2O/95% H_2O), phosphate buffer (30 μL of 200 mM solution in 5% D_2O/95% H_2O, pH 5.4), **Ia** single strand stock solution (184.2 μL of 5.92 mM solution in 5% D_2O/95% H_2O), **Ib** single strand stock solution (155.6 μL of 6.42 mM solution in 5% D_2O/95% H_2O) and 5% D_2O/95% H_2O (44.2 μL). An aliquot of ^{15}N-**1** (23.1 μL of 1.41 mg, 1.82 μmol dissolved in 40.0 μL) was added to give a reaction mixture of volume 439.1 μL and reactant concentrations of duplex **I** (2.39 mM) and ^{15}N-**1** (2.39 mM). The stock solution of the duplex contained a high amount of acetate impurity (from salting out the sequence) that was not present for the kinetic study. The concentration of acetate in the final NMR solution was estimated to be ~250 mM, based on the relative integrals of the acetate and thymine methyl resonances in the ^{1}H NMR spectrum.

pH Measurements: The pH of the solutions was measured on a Shindengen pH Boy-P2 (su19A) pH meter and calibrated against pH buffers of pH 6.9 and 4.0. The solution (5.0 μL) was placed on the electrode surface and the pH was recorded. These aliquots were not returned to the bulk solution (as the electrode leaches Cl^-). Adjustments in pH were made using 0.04 M, 0.2 M, and 1.0 M $HClO_4$ in 5% D_2O in H_2O, or 0.04 M, 0.2 M, and 1.0 M NaOH in 5% D_2O in H_2O.

NMR spectroscopy: The NMR spectra were recorded on a Varian UNITY-INOVA-600 MHz spectrometer (^{1}H, 599.92 MHz; ^{15}N, 60.79 MHz). The ^{1}H NMR chemical shifts are internally referenced to TSP and the ^{15}N chemical shifts externally referenced to $^{15}NH_4Cl$ (1.0 M in 1.0 M HCl in 5% D_2O in H_2O). The ^{1}H spectra were acquired with water suppression using the WATERGATE sequence.[35] The two-dimensional [^{1}H,^{15}N] heteronuclear single quantum coherence (HSQC) NMR spectra (decoupled with the GARP-1 sequence during the acquisition) were recorded using the sequence of Stonehouse et al.,[36] as described previously.[37] Samples were not spun during the acquisition of data. All samples (including buffers, acids etc.) were prepared so that there was a 5% D_2O/95% H_2O concentration (for deuterium lock but with minimal loss of signal as a result of deuterium exchange). Spectra were recorded at 298 K, and the sample was maintained at this temperature when not immersed in the NMR probe. Typically for 1D ^{1}H spectra, 64 or 128 transients were acquired using a spectral width of 12 kHz and a relaxation delay of 1.5 s. For kinetics studies involving [^{1}H,^{15}N]-HSQC NMR spectra, 4 or 8 transients were collected for 128–160 increments of t_1 (allowing spectra to be recorded on a suitable timescale for the observed reaction), with an acquisition time of 0.152 s, spectral widths of 4 kHz in f_2 (1H) and 1.8 kHz in f_1 (^{15}N). 2D spectra were completed in 14–36 minutes. The 2D spectra were processed by using Gaussian weighting functions in both dimensions, and zero-filling by $\times 2$ in the f_1 dimension. The 2D NOESY spectrum was acquired at 298 K with 24 transients over a ^{1}H spectral width of 20 ppm (12.0 kHz) into 4096 data points for each of 1024 t_1 increments by using a mixing time of 150 ms and a recycle delay of 2 s. The solvent signal was suppressed using a WATERGATE[35] routine and the acetate peak was removed by digital filtering. Linear prediction methods were employed to enhance the signal to noise ratio of the spectra during processing with VNMR software.

Data analysis: The kinetic analysis of the reactions were undertaken by measuring peak volumes in the Pt–NH_3 regions of the [^{1}H,^{15}N]-HSQC spectra by using the Varian VNMR software package and calculating relative concentrations of the various {Pt_2} species at each time point, as described previously.[12] Peak volumes were determined using an identical vertical scale and threshold value in successive spectra. All species, other than ^{15}N-**1**, gave rise to two [^{1}H,^{15}N]-HSQC peaks in the Pt–NH_3 region, due to non equivalent {PtN_3Y} groups. Overlap between peaks was significant. In cases where only one of the pair was overlapped (e.g. the peak for the non-aquated {PtN_3Cl} group of the monoaqua-monochloro species (**2**) is coincident with the peak for **1**),[11, 12] reliable intensities were obtained by doubling the volume of the second (discrete) peak. Adjustment for overlap of other peaks is fully explained in the Supporting Information. Most species also gave rise to resolved peaks in the Pt–NH_2 region of the [^{1}H,^{15}N]-HSQC correlation spectra and comparison of the time dependent changes in the two regions was used to confirm the peak assignments. The appropriate differential equations were integrated numerically, and rate constants determined by a non linear optimization procedure by using the program SCIENTIST (Version 2.01, MicroMath). The errors represent one standard deviation. In all cases the data were fit appropriate to first- and second-order rate equations. Minima were found using simulations, and by gradually optimizing the input parameters, fixing some, while others were refined, then finally allowing all parameters to be refined simultaneously. The kinetic models are provided in the Supporting Information.

Acknowledgements

This work was supported by the Australian Research Council, US National Institutes of Health (RO1-CA78754), US National Science Foundation (INT-9805552 and CHE-9615727) and the American Cancer Society (RPG(8)9–002–11-CDD). We thank Dr W. Barklage for the preparation of ^{15}N-**1** and Dr Greg Pierens (Griffith University) for assistance with the NMR experiments.

[1] N. Farrell, Y. Qu, U. Bierbach, M. Valsecchi, E. Menta in *Cisplatin: Chemistry and Biochemistry of a Leading Anticancer Drug* (Ed.: B. Lippert), VCHA, Zurich, **1999**, pp. 479–496.
[2] N. Farrell, *Comments Inorg. Chem.* **1995**, *16*, 373–389.
[3] P. M. Calvert, M. S. Highley, A. N. Hughes, E. R. Plummer, A. S. T. Azzabi, M. W. Verrill, M. G. Camboni, E. Verdi, A. Bernareggi, M. Zucchetti, A. M. Robinson, J. Carmichael, A. H. Calvert, *Clin. Cancer Res.* **1999**, *5*, 3796.
[4] G. Pratesi, P. Perego, D. Polizzi, S. C. Righetti, R. Supino, C. Caserini, C. Manzotti, F. C. Giuliani, G. Pezzoni, S. Tognella, S. Spinelli, N. Farrell, F. Zunino, *Br. J. Cancer* **1999**, *80*, 1912–1919.
[5] P. Perego, C. Caserini, L. Gatti, N. Carenini, S. Romanelli, R. Supino, D. Colangelo, I. Viano, R. Leone, S. Spinelli, G. Pezzoni, C. Manzotti, N. Farrell, F. Zunino, *Mol. Pharmacol.* **1999**, *55*, 528–534.
[6] Y. Qu, H. Rauter, A. P. Soares Fontes, R. Bandarage, L. R. Kelland, N. Farrell, *J. Med. Chem.* **2000**, *43*, 3189–3192.

  0947-6539/03/0903-0724 $ 20.00+.50/0

[7] N. Farrell in *Platinum Based Drugs in Cancer Chemotherapy* (Eds.: L. R. Kelland, N. Farrell), Humana Totawa, NJ, **2000**, pp. 321–338.
[8] H. Rauter, R. Di Domenico, E. Menta, A. Oliva, Y. Qu, N. Farrell, *Inorg. Chem.* **1997**, *36*, 3919–3927.
[9] T. D. McGregor, A. Hegmans, J. Kasparková, K. Neplechová, O. Nováková, H. Penazová, O. Vrána, V. Brabec, N. Farrell, *J. Biol. Inorg. Chem.* **2002**, *7*, 397–404.
[10] V. Brabec, J. Kasparková, O. Vraná, O. Nováková, J. W. Cox, Y. Qu, N. Farrell, *Biochemistry* **1999**, *38*, 6781–6790.
[11] M. S. Davies, J. W. Cox, S. J. Berners-Price, W. Barklage, Y. Qu, N. Farrell, *Inorg. Chem.* **2000**, *39*, 1710–1715.
[12] J. W. Cox, S. J. Berners-Price, M. S. Davies, Y. Qu, N. Farrell, *J. Am. Chem. Soc.* **2001**, *123*, 1316–1326.
[13] S. J. Berners-Price, K. J. Barnham, U. Frey, P. J. Sadler, *Chem. Eur. J.* **1996**, *2*, 1283–1291.
[14] Y. Chen, J. A. Parkinson, Z. Guo, T. Brown, P. J. Sadler, *Angew. Chem.* **1999**, *111*, 2192–2196; *Angew. Chem. Int. Ed.* **1999**, *38*, 2060–2063.
[15] P. del S. Murdoch, Z. Guo, J. A. Parkinson, P. J. Sadler, *J. Biol. Inorg. Chem.* **1999**, *4*, 32–38.
[16] Y. Zou, B. Van Houten, N. Farrell, *Biochemistry* **1994**, *33*, 5404–5410.
[17] J. A. Parkinson, Y. Chen, P. del S. Murdoch, Z. Guo, S. J. Berners-Price, T. Brown, P. J. Sadler, *Chem. Eur. J.* **2000**, *6*, 3636–3644.
[18] F. Reeder, Z. Guo, P. del S. Murdoch, A. Corazza, T. W. Hambley, S. J. Berners-Price, J. C. Chottard, P. J. Sadler, *Eur. J. Biochem* **1997**, *249*, 370–382.
[19] S. J. Berners-Price, T. A. Frenkiel, U. Frey, J. D. Ranford, P. J. Sadler, *J. Chem. Soc. Chem. Commun.* **1992**, 789–791.
[20] M. S. Davies, S. J. Berners-Price, D. S. Thomas, N. Farrell, unpublished results. The $^{1}H/^{15}N$ peaks (**3b**/**4b**) of the uncoordinated end of the two monofunctional adducts could be discriminated in the analogous reaction between ^{15}N-**1** and **I** in the presence of 250 mM acetate.
[21] Molecular models were constructed to visualise the different local environments of the Pt−$(NH_3)_2$ groups in the two conformers and aided in the interpretation of the [^{1}H,^{15}N]-HSQC NMR spectra and these are provided as Supporting Information. The NOESY spectrum provides evidence for *syn* orientations for several of the bases in the bifunctional adduct, indicating that these models based on B-form DNA are not valid representations of the 1,4-interstrand cross-link. However, the close contact (hydrogen bonds) between the ammine ligands of **1** and the duplex are assumed to be largely independent of these local distortions from B-form DNA.
[22] J. Kasparková, J. Zehnulova, N. Farrell, V. Brabec, *J. Biol. Chem.* **2002**, in press.
[23] Y. Qu, N. J. Scarsdale, M. C. Tran, N. Farrell, *J. Biol. Inorg. Chem.* **2002**, *8*, 19–28.
[24] Y. Qu, N. Farrell, unpublished results.
[25] M. S. Davies, S. J. Berners-Price, J. W. Cox, N. Farrell, *Chem. Commun.* **2003**, 122–123.
[26] M. S. Davies, S. J. Berners-Price, T. W. Hambley, *Inorg. Chem.* **2000**, *39*, 5603–5613.
[27] H. Sugiymaa, I. Saito, *J. Am. Chem. Soc.* **1996**, *118*, 7063–7068.
[28] J. Kasparková, O. Nováková, O. Vrána, N. Farrell, V. Brabec, *Biochemistry* **1999**, *38*, 10997–11005.
[29] R. Zaludová, A. Zakovská, J. Kasparková, Z. Balcarová, V. Kleinwächter, O. Vrána, N. Farrell, V. Brabec, *Eur. J. Biochem.* **1997**, *246*, 508–517.
[30] J. Kasparková, N. Farrell, V. Brabec, *J. Biol. Chem.* **2000**, *275*, 15789–15798.
[31] S. J. Berners-Price, M. S. Davies, A. Hegmans, D. S. Thomas, N. Farrell, unpublished results.
[32] J. W. Cox, PhD thesis, Virginia Commonwealth University (Richmond, VA), **2000**.
[33] T. D. McGregor, W. Bousfield, Y. Qu, N. Farrell, *J. Inorg. Biochem.* **2002**, *91*, 212–219.
[34] G. Kallansrud, B. Ward, *Anal. Biochem.* **1996**, *236*, 134–138.
[35] M. Piotto, V. Saudek, V. Sklenar, *J. Biomol. NMR* **1992**, *2*, 661–665.
[36] J. Stonehouse, G. L. Shaw, J. Keeler, E. D. Laue, *J. Mag. Res. Ser. A* **1994**, *107*, 174–184.
[37] M. S. Davies, S. J. Berners-Price, T. W. Hambley, *J. Am. Chem. Soc.* **1998**, *120*, 11380–11390.

Received: July 23, 2002 [F4274]

  0947-6539/03/0903-0725 $ 20.00+.50/0